Influence of concentration, type and particle size of fillers on the dynamic mechanical behaviour of elastomeric HTPB binder

Dr. Manfred A. Bohn*, Mauricio Ferrapontoff Lemos**,*, Günter Mussbach***,*

Manfred.Bohn@ict.fraunhofer.de

* Fraunhofer Institut für Chemische Technologie (ICT), D-76318 Pfinztal, Germany
** Brazilian Navy Research Institute, Rio de Janeiro, RJ, 21931-090, Brazil
*** Bayern-Chemie GmbH, 84544 Aschau am Inn, Germany

Presentation on the NDIA IMEMTS, event # 8550
Presentation reference number 20069
(Insensitive Munitions & Energetic Materials Technology Symposium)
April 23-26, 2018
Portland, Oregon, USA

Fraunhofer ICT

Overview

Introduction

Objective

Substances

Manufacture of samples
- Mixing of ingredients
- Achieving homogenous distribution of filler in binder

Characterisation methods – Röntgen (X-ray)-CT, SEM, DMA, $T_{g,DMA}(f)$, EMG modelling

Results
- Parameterisation of the shift of glass-rubber transition (GRT) temperature $T_{g,DMA}$ with the DMA deformation frequency f
- Quantification of loss factor tanδ with EMG (exponentially modified Gauss distribution)

Discussion

Conclusions

Fraunhofer ICT

Introduction

What is known

In a series of investigations it was found that the second evident peak in the DMA loss factor curve of HTPB bonded composite RPs and PBXs changes in shape with composition. Bonded AP gives a clear established peak, HMX and RDX develop a smaller one; and with high degree of filling it is present as a shoulder only, see HX2.

This second peak is very ageing sensitive. It can be indicative for (1) de-wetting between filler and binder; (2) formation of a polymeric shell around the particle.

This means intermolecular inter-actions (pure sterical, energetic) show influence on second peak and on the shape of loss factor as a whole.

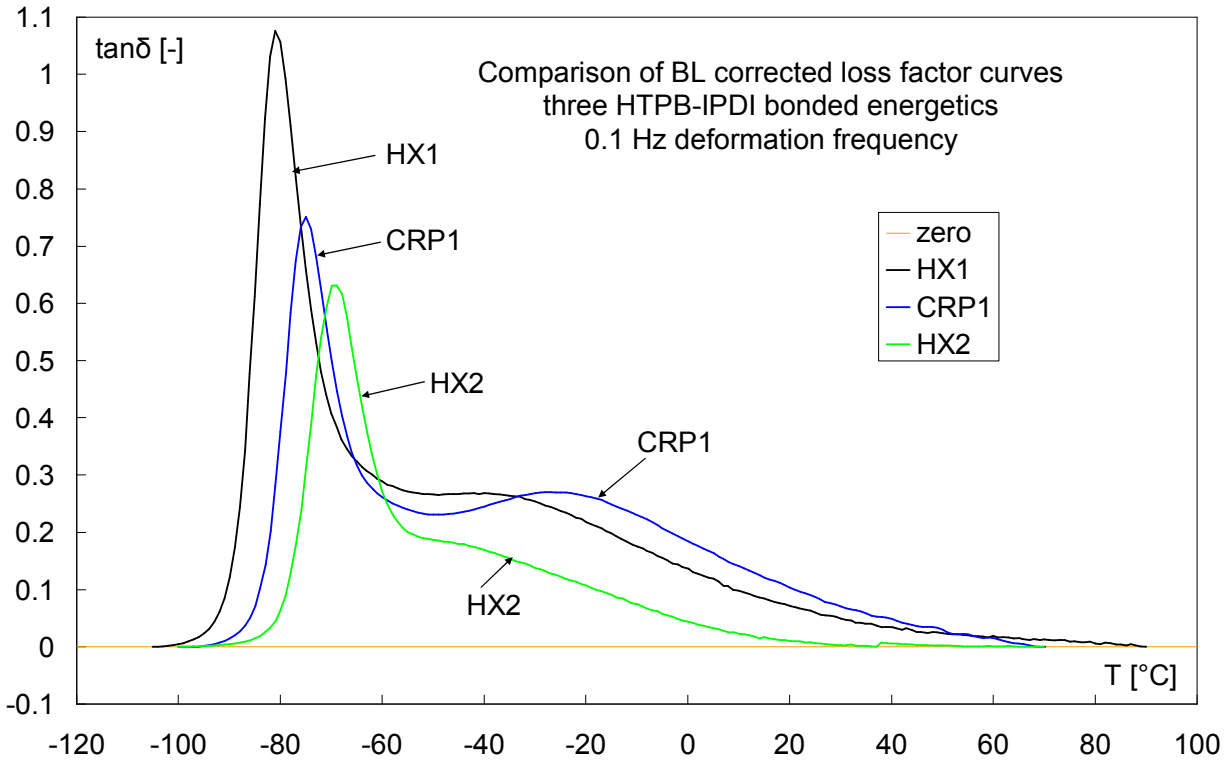

The principle structure / shape of loss factor is the same with all three compounds. Always two evident maxima.
Composition in mass-%
CRP. HTPB-IPDI (12), AP (78), Al (6), DOA (4, 25% of binder)
HX1: HTPB-IPDI (12), RDX (80), DOA (8, 40% of binder)
HX2: HTPB-IPDI (14), HMX (85), DOA (1, 6.7% of binder)

The plasticizer content determines mainly the position and the height of first peak.

Fraunhofer ICT

Objective

Experimental investigation on the influence of concentration and type of fillers on the shape and intensity of loss factor and on its shift with deformation frequency.

Three types of fillers with two particle sizes each are used in formulations with standardized binder matrix.

Fraunhofer ICT

Substances – binder ingredients for the investigated formulations

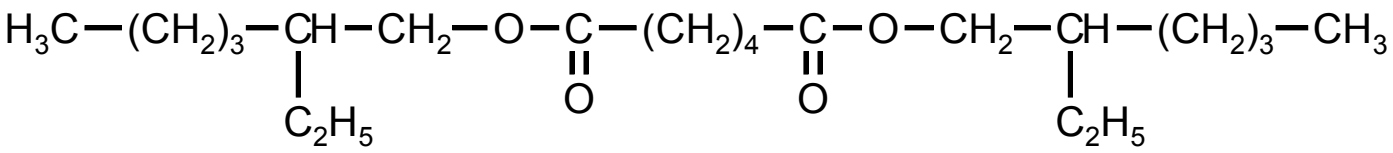

Di-iso-octyl adipate
DOA (plasticizer)

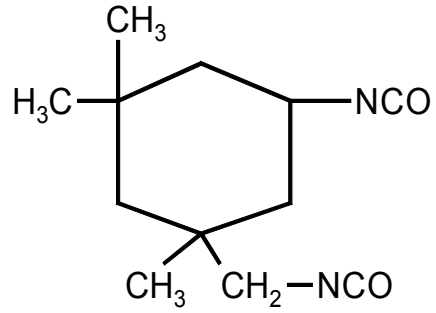

Isophorone diisocyanate
IPDI (cross-linker)

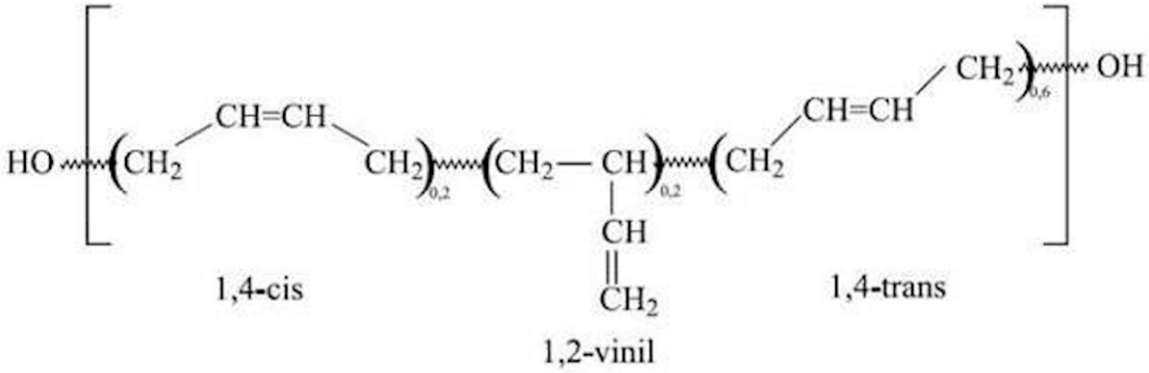

Hydroxyl-terminated polybutadiene
HTPB (pre-polymer)

HTPB + IPDI form the elastomer binder as polyurethane

All formulations made with equivalent ratio Req (NCO / OH) = 0.85 (RP type curing)
Antioxidant added to protect the HTPB
No curing catalyst added. Equal curing at 60°C, 130 h (5d, 10h)
Always with 5 mass-% plasticizer (DOA) in binder

Fraunhofer ICT

Substances – fillers AP (ammonium perchlorate) and RDX, two particle sizes

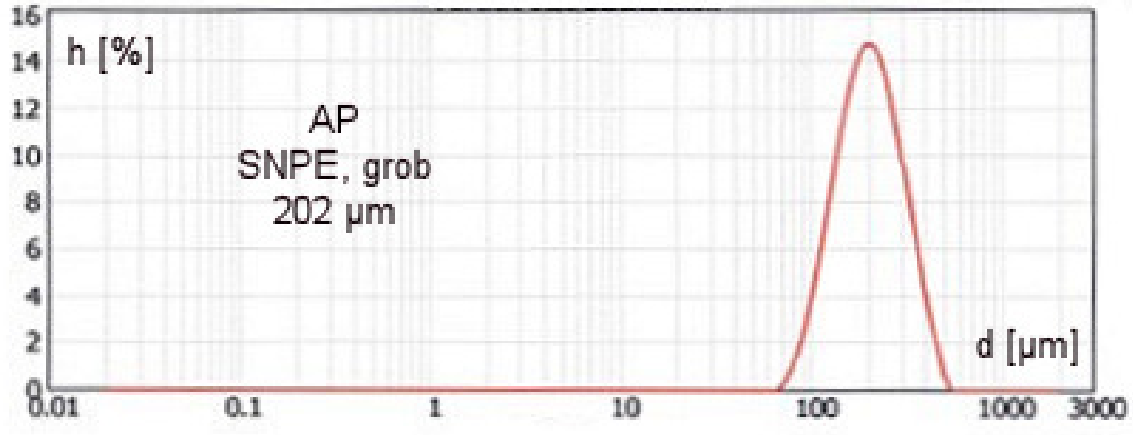

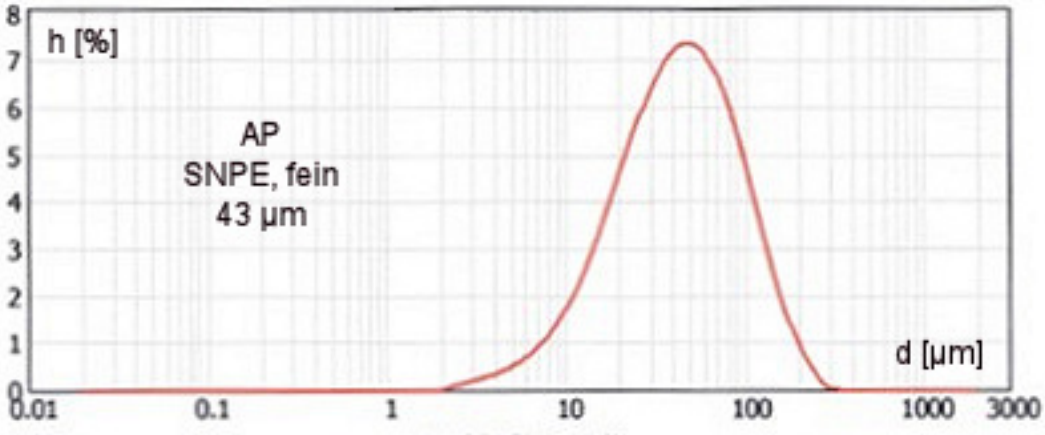

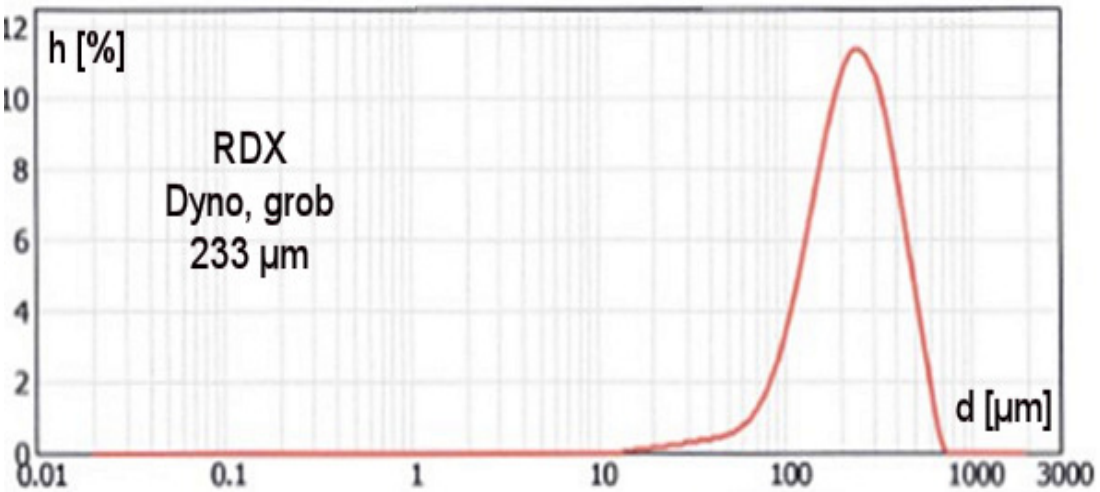

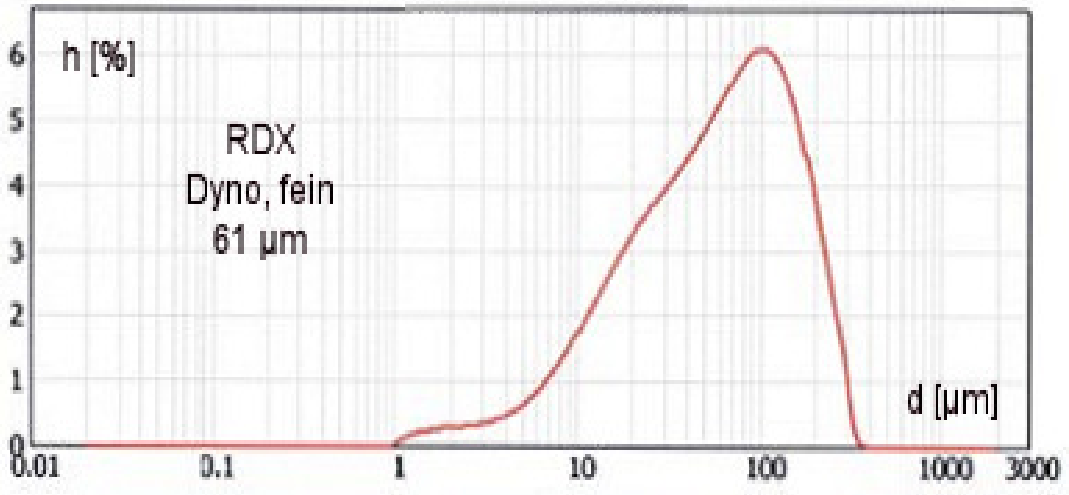

grob = coarse

fein = fine (small)

Fraunhofer ICT

Substances – filler Al (aluminium), two particle sizes

Aluminium - Al

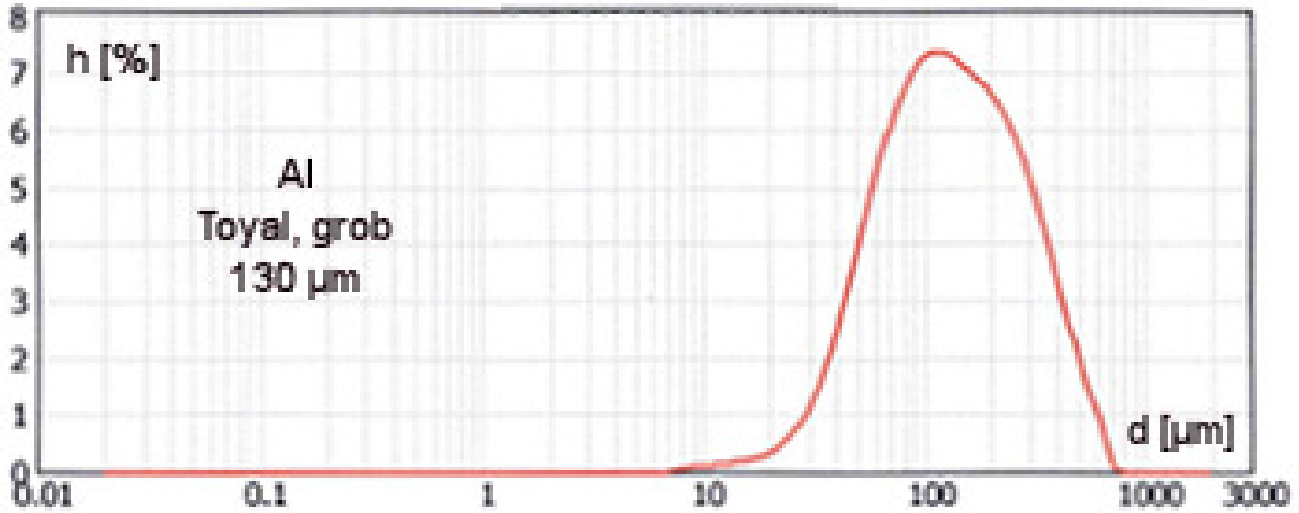

grob = coarse

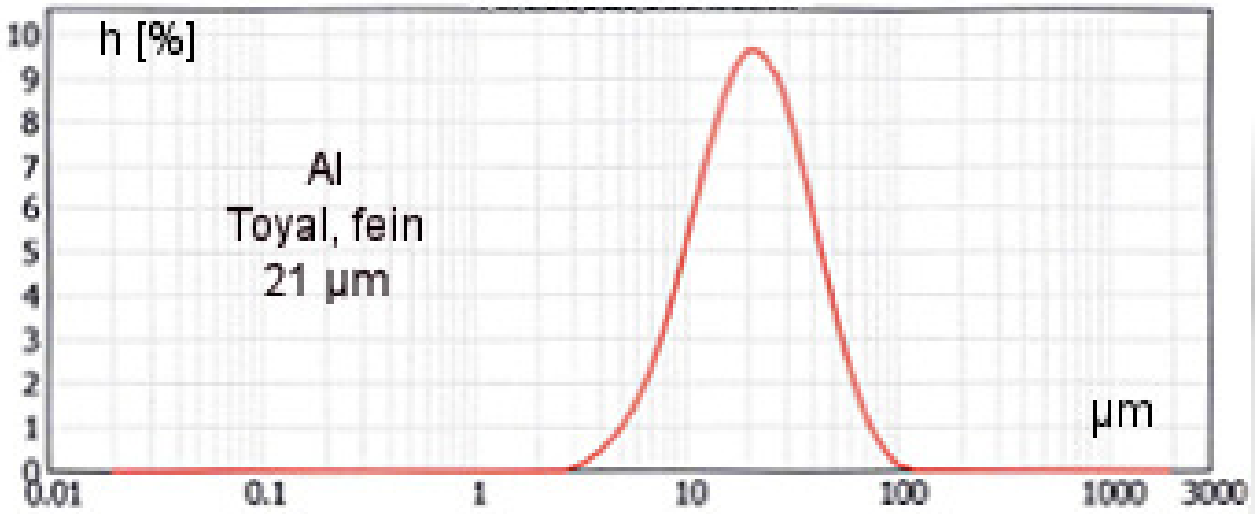

fein = fine

Fraunhofer ICT

Manufacturing of the samples

With each of the six filler substances formulations were manufactured
Different filler contents: 20 mass-%, 40 mass-%, 60 mass-%

The formulations were mixed with a planetary-rotary mixer (PRM) of type ‘Thinky mixer’.
Conditions: 1600 rpm, p = 30 mbar = 3 kPa, mixing in the way to keep T < 40°C.

Pouring the final mix in small glass bottles with lid.

It is known:
Even with highly filled binders a certain sedimentation of fillers is observed.
Sedimentation will happen with such low content of fillers for sure.

To get useful results with DMA, the samples must be homogenous.

Therefore, a special curing method was developed.
The curing was done with a turning device mounted in the curing oven.

Fraunhofer ICT

Samples - Maunfacturing - curing - characterisation

HTPB
+
plasticizer

Filler

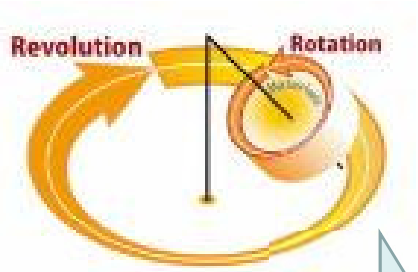

R_{eq}=NCO/OH = 0.85

Mix procedure in the way to keep T < 40°C

Using planetary – rotary mixer called ‘Thinky mixer’

Addition of IPDI at end of main mixing. One minute further mixing.

Curing in oven at 60°C with turning device

After curing analysis with DMA

Fraunhofer ICT

Turning device to achieve homogenoues filler distribution during curing

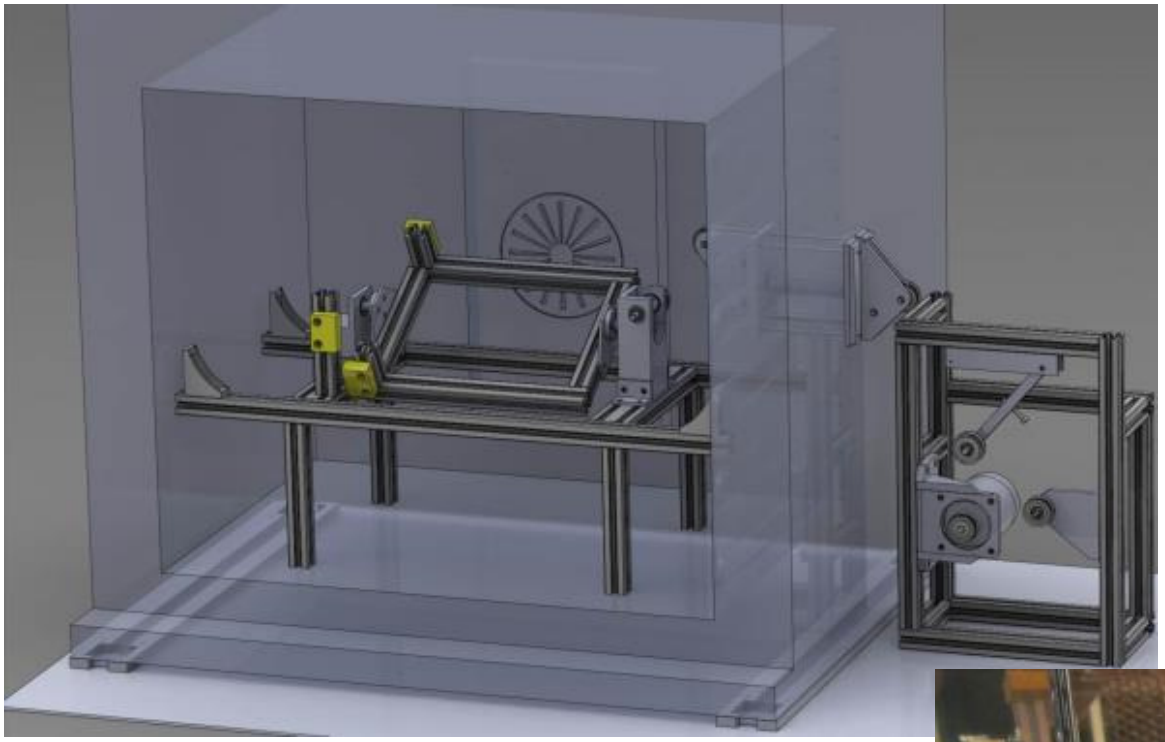

Turning device manufactured at Fraunhofer ICT, mounted in circulating air oven. Motor drive (brushless) outside of oven.
Turning time for 180°: 3 seconds
Hold time: 1 minutes (adjustable).
Important: it may not be a continuous turning.

’Construction‘ (artificial) photo

Real photograph

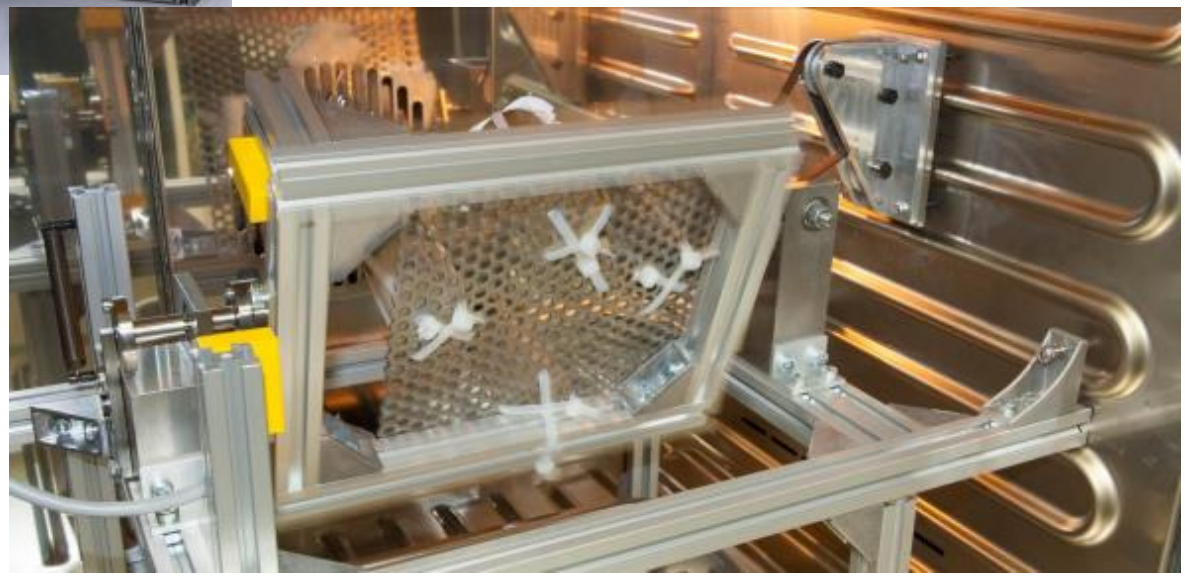

Fraunhofer ICT

Characterisation methods

Röntgen (X-ray)-micro-CT

(Wilhelm Conrad Röntgen discovered the effect, he got the first Nobel price in Physics 1901)
With computer tomography of type Micro-CT in-vivo Skyscan 1076 of company Bruker, Germany, the cured samples were tested on the quality of filler distribution.

SEM

Scanning electron microscopy, type Supra 55VP, ZEISS, Germany was used to analyse the surface and shape of the particles: rough, smooth, irregular, spherical.

DMA (dynamic mechanical analysis) - complex shear modulus and loss factor

DMA performed in torsion mode which provides the complex shear modulus. Used deformation frequencies: 0.1Hz, 1Hz, 10Hz and 30Hz. T-range -100°C to +70°C
The glass-rubber transition (GRT) temperatures $T_{g,DMA}$ were determined from both evident maxima in the loss factor curve $\tan\delta(T) = G''(T)/G'(T)$ by fitting a polynomial of degree 3 carefully at each of the two maxima ranges, selecting the data range for optimal fitting.

EMG – Quantification of baseline corrected (BLC) loss factor curve

The peaks of loss factor curve correspond the binder parts with different mobility of the polymer chains For quantification of these curve parts so-called EMG functions have been applied to baseline corrected loss factor. **The total loss factor curve of HTPB needs three EMG functions.**
(EMG: exponentially modified Gauss distribution)

Fraunhofer ICT

Testing on homogenous distribution of fillers

Verification of the homogenous distribution of the fillers during the curing of HTPB-IPDI binder with 20 mass-% AP, achieved by the turning device.

Normal photograph of sample
20 mass-% AP

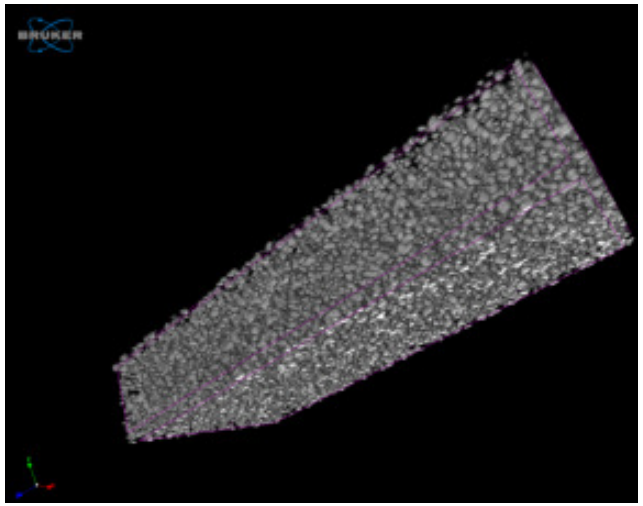

Röntgen (X-ray)-Micro-CT
20 mass-% AP

Fraunhofer ICT

Typical DMA measurement result on loss factor – filler is AP

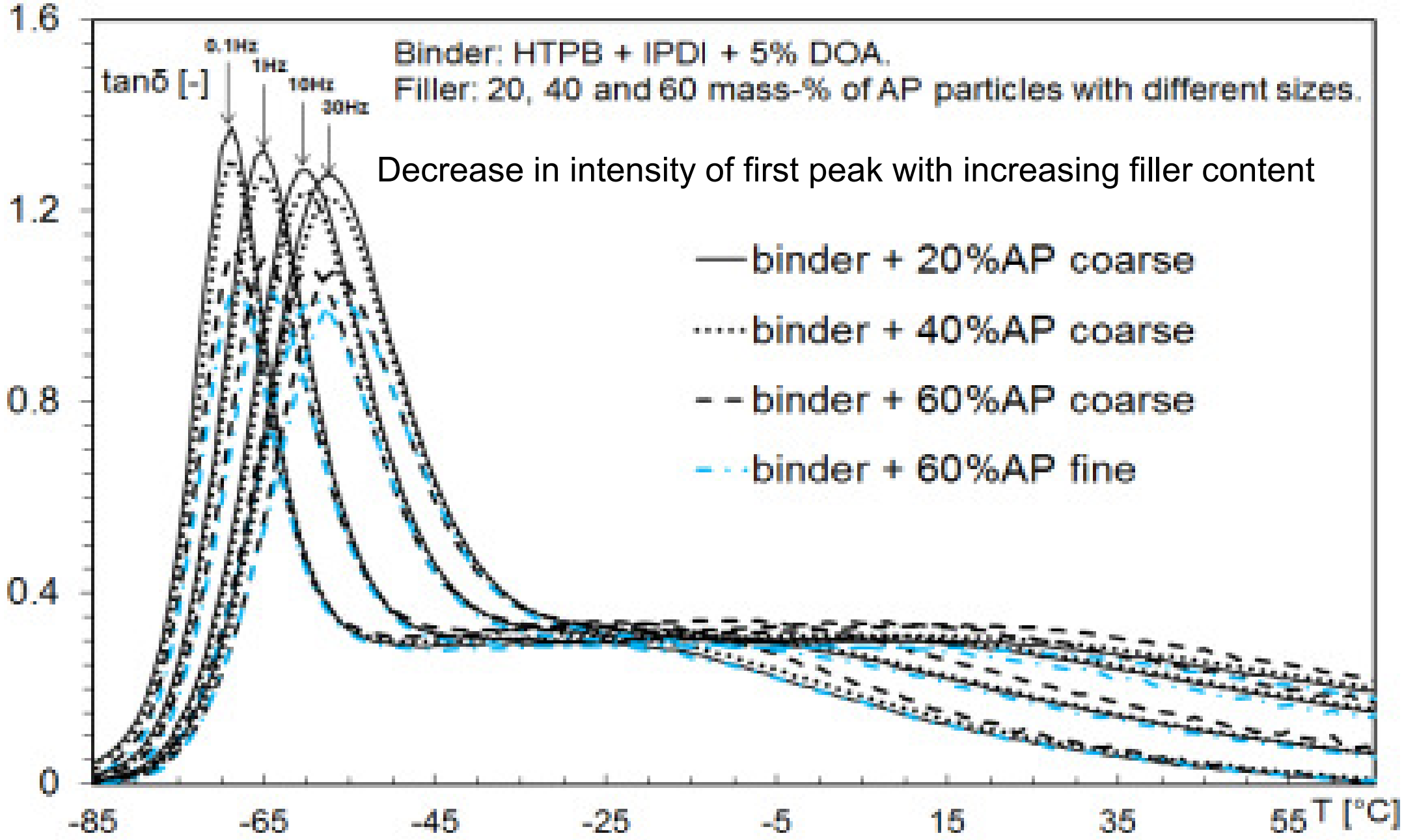

Fraunhofer ICT

Assignment of peaks to binder parts – first main peak

The first evident peak gives the GRT temperature T_g^{unr}

The first peak is created by the binder part with **non**-hindered chain mobility. It is the 'un-restricted' glass-rubber transition.

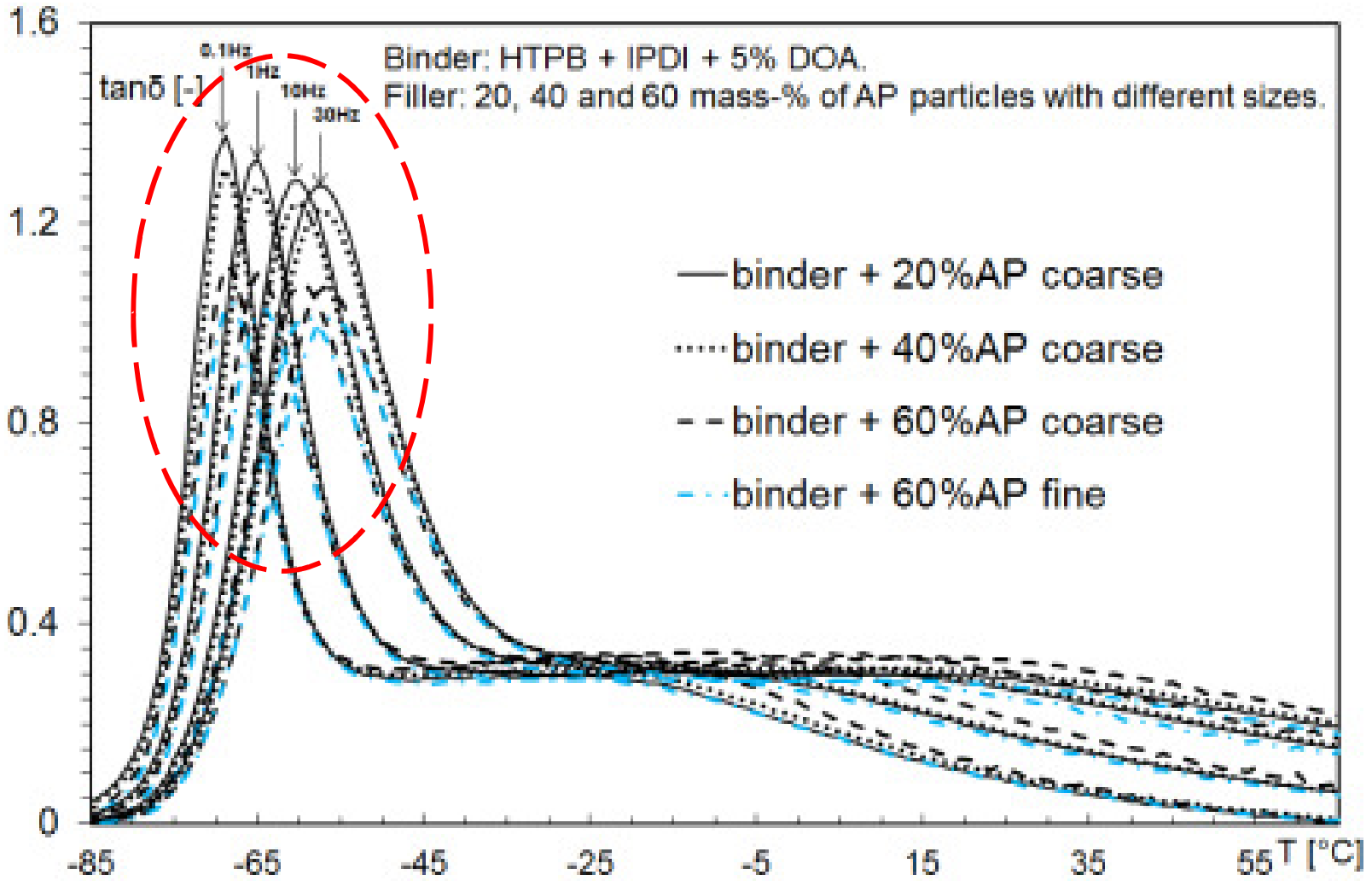

The non-hindered binder part is formed by the polymer chains of HTPB not restricted in their mobility.

Fraunhofer ICT

Assignment of peaks to binder parts – second main peak

The second evident peak gives the GRT temperature T_g^{res}

The second peak is created by the binder part with hindered chain mobility. It is the 'restricted' glass-rubber transition.

These mobility hindered binder parts are found
(1) around the IPDI cross-linking ranges
(2) with binder chains, which are mobility-restricted by the interaction with the filler, in part geometrically-sterically in part by energetic interactions..

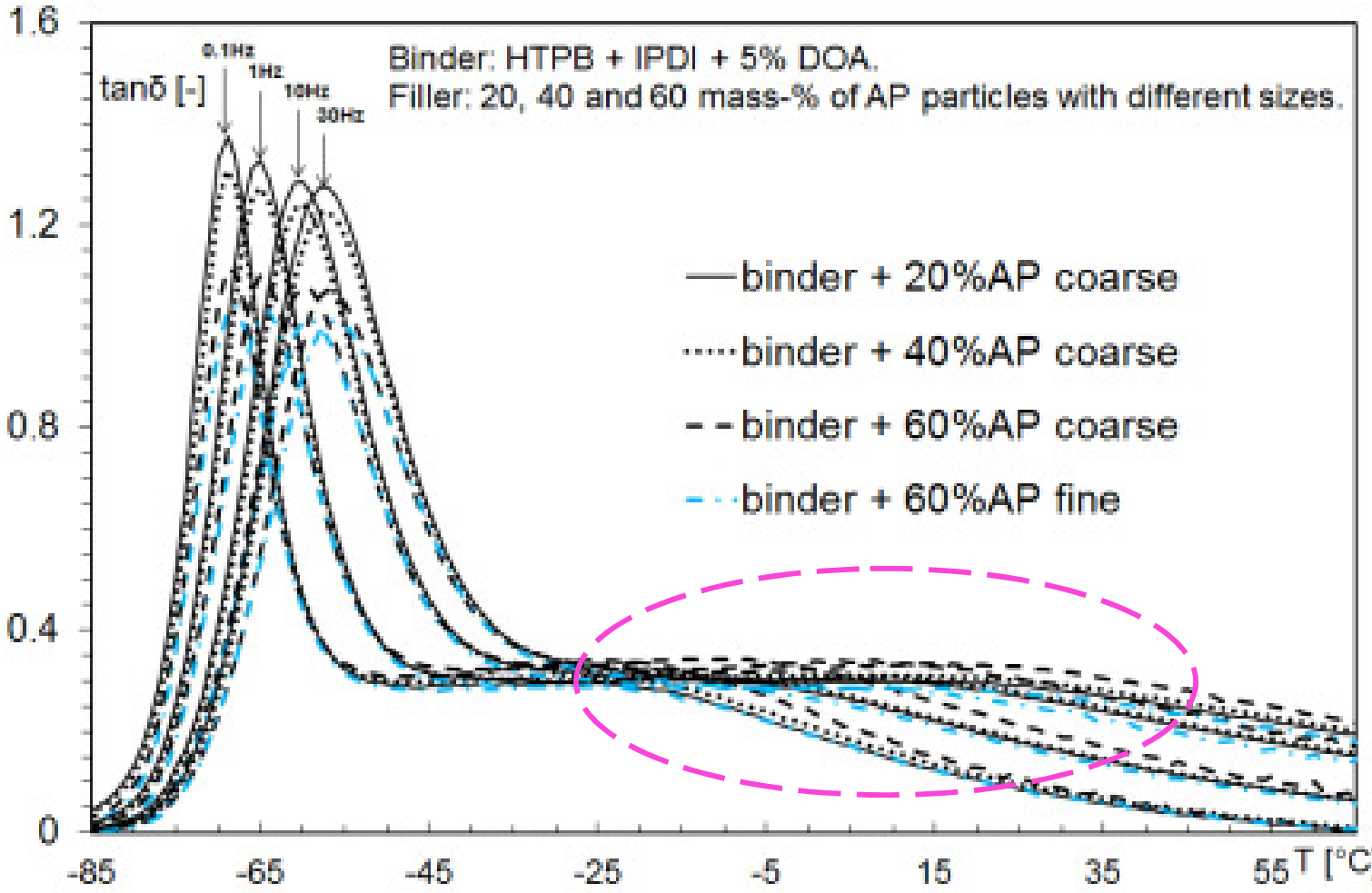

Fraunhofer ICT

Changes in loss factor – caused by AP and RDX

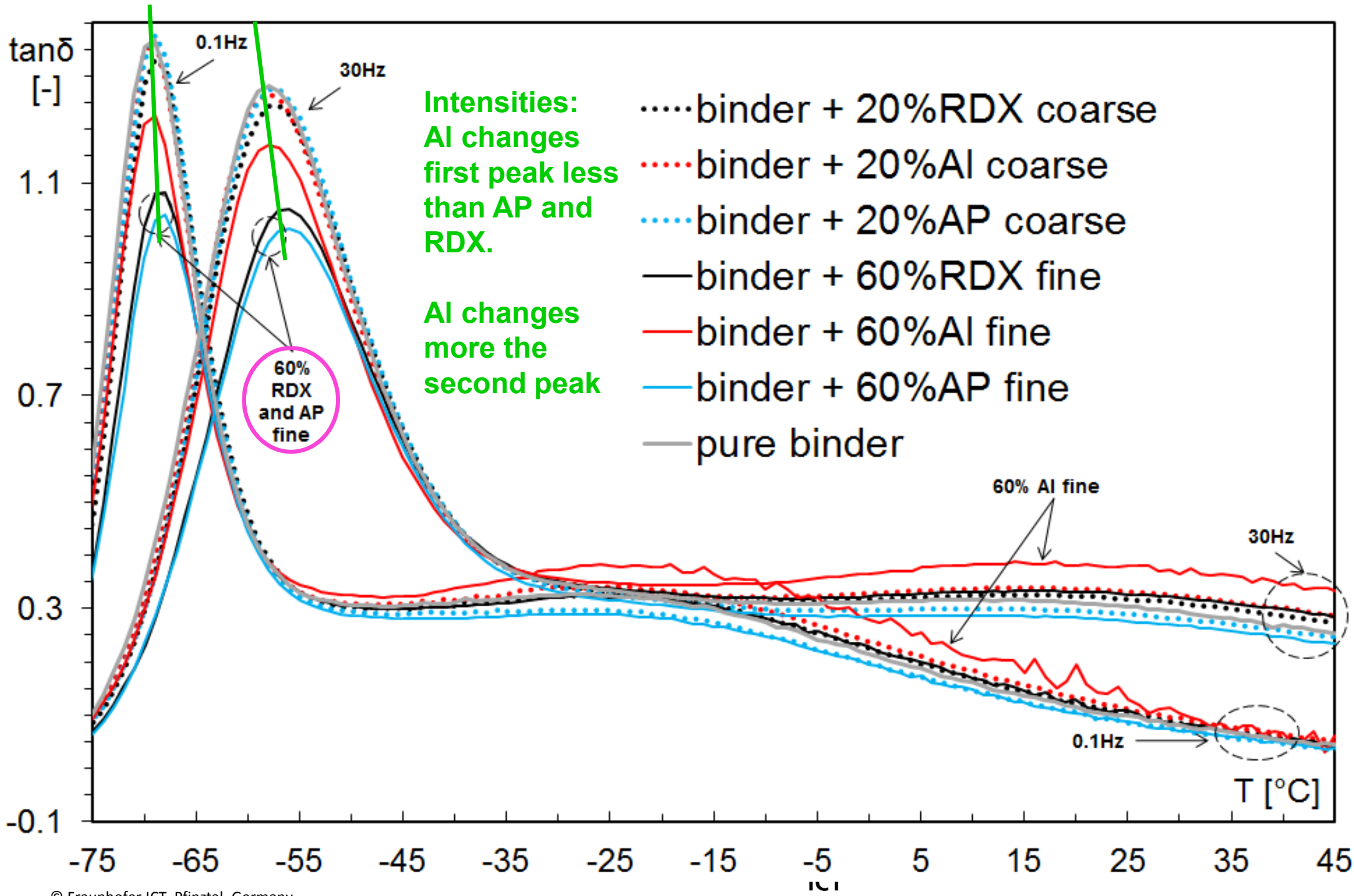

Parameterisation of shift of $T_{g,DMA}$ with deformation frequency f

Both the glass-rubber transition temperatures T_g^{unr} and T_g^{res} are determined from the loss factor curves.
For this a polynomial of degree 3 was fitted in the maxima ranges to determine the maxima data. To take the values just from measured temperature interval data is not precise enough.

Parameterisation of shift according to Arrhenius with following equation

$$f = f_0 \cdot \exp\left(-\frac{Ea_f}{R \cdot T_g(f)}\right)$$

This shift with temperature is not based on free volume effect, it is an inertia effect and interaction energy determined

f	applied deformation frequency [Hz];
f_0	pre-exponential factor [Hz];
Ea_f	activation energy for the shift of T_g by strain rate hardening [kJ·mol^{-1}];
R	general gas constant [8.31441 J·K^{-1} mol^{-1}];
T_g	glass-rubber transition temperature [K] as function of deformation frequency

The obtained activation energy is a measure for the internal interaction energy in the binder.

Fraunhofer ICT

Parameterisation of shift of $T_{g,DMA}$ with deformation frequency f

Parameterisation of shift according to **modified Arrhenius** with following equation

$$f = f_{0M} \cdot \exp\left(-\frac{Ea_{0M}}{R \cdot (T_g(f) - T_{0M})} \right)$$

The modified Arrhenius equation is **completely congruent** to the WLF equation !

$$\lg\left(a_T(T,Tr)\ [-]\right) = \lg\left(\frac{f(Tr)}{f(T)}\right) = -\frac{C_1 \cdot (T - Tr)}{C_2 + (T - Tr)}$$

f	applied deformation frequency [Hz];
f_{0M}	pre-exponential factor [Hz];
Ea_{0M}	activation energy for the shift of T_g by strain rate hardening [kJ·mol^{-1}];
R	general gas constant [8.31441 J·K^{-1} mol^{-1}];
T_g	glass-rubber transition temperature [K] as function of deformation frequency
T_{0M}	mobility freezing reference temperature, identical to T_∞ of WLF equation (T zero mobility)

$$Ea_{0M} = R \cdot C_1 \cdot C_2 / \lg(e) \qquad T_{0M} = Tr - C_2 = T_\infty$$

The Arrhenius activation energy is proportional to the second WLF invariant $C_1 \cdot C_2$

See: Manfred A. Bohn, ***The connection between WLF equation and Arrhenius equation***. Proceedings 21th International Seminar NTREM (New Trends in Research of Energetic Materials), April 18-20, **2018**. Pages 64 to 81. University of Pardubice, Pardubice, Czech Republic.
For a copy send me an e-mail: bo@ict.fhg.de

Fraunhofer ICT

Activation energies from strainrate shift of first peak (un-restricted GRT with T_g^{unr})

sample	T_g^{unr}				difference to reference				Ea_f^* [kJ.mol^{-1}]	ln(f_0 [Hz])
	0.1Hz	1Hz	10Hz	30Hz	0.1Hz	1Hz	10Hz	30Hz		
only binder	-69.42	-65.58	-60.72	-57.95	***+ means to higher temp.***				**180.7**	45.43
20 % AP coarse	-68.86	-65.24	-60.28	-57.51	*0.56*	*0.34*	*0.44*	*0.44*	**182.6**	45.79
40 % AP coarse	-68.78	-65.04	-60.11	-57.27	*0.64*	*0.54*	*0.61*	*0.68*	**180.9**	45.34
60 % AP coarse	-68.63	-64.76	-59.62	-56.74	*0.79*	*0.82*	*1.10*	*1.21*	**175.4**	43.91
60 % AP fine	-68.29	-64.38	-59.06	-56.16	*1.13*	*1.20*	*1.66*	*1.79*	**172.3**	43.04
20 % RDX coarse	-68.95	-65.02	-60.09	-57.37	*0.47*	*0.56*	*0.63*	*0.58*	**179.8**	45.07
40 % RDX coarse	-68.97	-65.01	-59.91	-57.22	*0.45*	*0.57*	*0.81*	*0.73*	**176.7**	44.30
60 % RDX coarse	-69.58	-64.28	-59.02	-55.94	*-0.16*	*1.30*	*1.70*	*2.01*	**154.9**	38.78
60 % RDX fine	-69.44	-64.56	-59.19	-56.19	*-0.02*	*1.02*	*1.53*	*1.76*	**158.6**	39.71
20 % Al coarse	-68.90	-65.65	-60.76	-57.91	*0.52*	*-0.07*	*-0.04*	*0.04*	**187.3**	47.05
20 % Al fine	-69.54	-65.71	-60.81	-57.95	*-0.12*	*-0.13*	*-0.09*	*0*	**179.1**	45.00
40 % Al fine	-69.23	-65.69	-60.71	-57.77	*0.19*	*-0.11*	*0.01*	*0.18*	**180.6**	45.34
60 % Al fine	-69.01	-65.56	-60.60	-57.80	*0.41*	*0.02*	*0.12*	*0.15*	**184.0**	46.18

AP-coarse: decrease in Ea with content increase
RDX-coarse: decrease in Ea with content in increase
Al –fine: increase in Ea with content increase; at change from coarse to fine a change in Ea

Fraunhofer ICT

Activation energies from strainrate shift of second peak (restricted GRT with T_g^{res})

sample	T_g^{res}				difference to reference				Ea_f [kJ.mol^{-1}]	ln(f_0 [Hz])
	0.1Hz	1Hz	10Hz	30Hz	0.1Hz	1Hz	10Hz	30Hz		
Only binder	-28.04	-13.65	2.52	10.87	***+ means to higher temp.***				**84.71**	17.06
20 % AP coarse	-29.42	-15.63	2.00	11.03	*-1.38*	*-1.98*	*-0.52*	*0.16*	**80.66**	16.33
40 % AP coarse	-28.33	-14.14	2.94	12.46	*-0.29*	*-0.49*	*0.42*	*1.59*	**81.25**	16.37
60 % AP coarse	-24.92	-11.96	4.22	14.98	*3.12*	*1.69*	*1.70*	*4.11*	**85.41**	17.03
60 % AP fine	-29.25	-16.82	0.23	8.49	*-1.21*	*-3.17*	*-2.29*	*-2.38*	**85.24**	17.31
20 % RDX coarse	-25.36	-12.23	4.57	14.24	*2.68*	*1.42*	*2.05*	*3.37*	**85.12**	17.00
40 % RDX coarse	-24.34	-10.94	6.36	15.75	*3.70*	*2.71*	*3.84*	*4.88*	**84.64**	16.82
60 % RDX coarse	-25.38	*Not good defined*			*2.66*			*Not good defined*		
60 % RDX fine	-24.05	-11.76	4.96	15.47	*3.99*	*1.89*	*2.44*	*4.60*	**86.13**	17.14
20 % Al coarse	-26.01	-11.7	6.13	15.09	*2.03*	*1.95*	*3.61*	*4.22*	**81.66**	16.29
20 % Al fine	-25.88	-12.44	3.76	13.54	*2.16*	*1.21*	*1.24*	*2.67*	**85.51**	17.10
40 % Al fine	-25.91	-11.74	4.35	11.32	*2.13*	*1.91*	*1.83*	*0.45*	**88.67**	17.74
60 % Al fine	-23.25	-10.33	7.38	15.8	*4.79*	*3.32*	*4.86*	*4.93*	**86.54**	17.14

AP-coarse: increase in Ea with content increase
RDX-coarse: no defined result, probably Ea stays rather constant with content increase
Al –fine: more constant Ea with content increase; at change from coarse to fine a change in Ea

Fraunhofer ICT

Modelling of loss factor curve of HTPB-IPDI with three EMGs

Quantification of the effects of fillers via exponentially modified Gauss distribution function

$$\tan\delta_{BLC} = td_0 + \sum_{i=1}^{N} \frac{A_i}{\tau_i} \cdot \frac{1}{2} \cdot \exp\left[0.5 \cdot \left(\frac{w_i}{\tau_i}\right)^2 - \frac{T - Tc_i}{\tau_i}\right] \cdot \left\{1 - \mathrm{erf}\left[-\frac{1}{\sqrt{2}}\left(\frac{T - Tc_i}{w_i} - \frac{w_i}{\tau_i}\right)\right]\right\}$$

Gauss distribution $$f_G(T) = \frac{A}{w \cdot \sqrt{2\pi}} \cdot \exp\left[-0.5 \cdot \left(\frac{T - Tc}{w}\right)^2\right]$$

exponential relaxation $$f_E(T) = \exp\left(-\frac{T}{\tau}\right)$$

EMG is mathematically a convolution between Gauss and exponential

One EMG has 4 parameters:

- Peak area, A_i;
- Half width at half height of Gauss function, w_i;
- Temperature in maximum of Gauss function, Tc_i;
- Relaxation parameter τ_i of exponential part, here also named as To.

Fraunhofer ICT

Modelling of loss factor curve of HTPB-IPDI with three EMGs

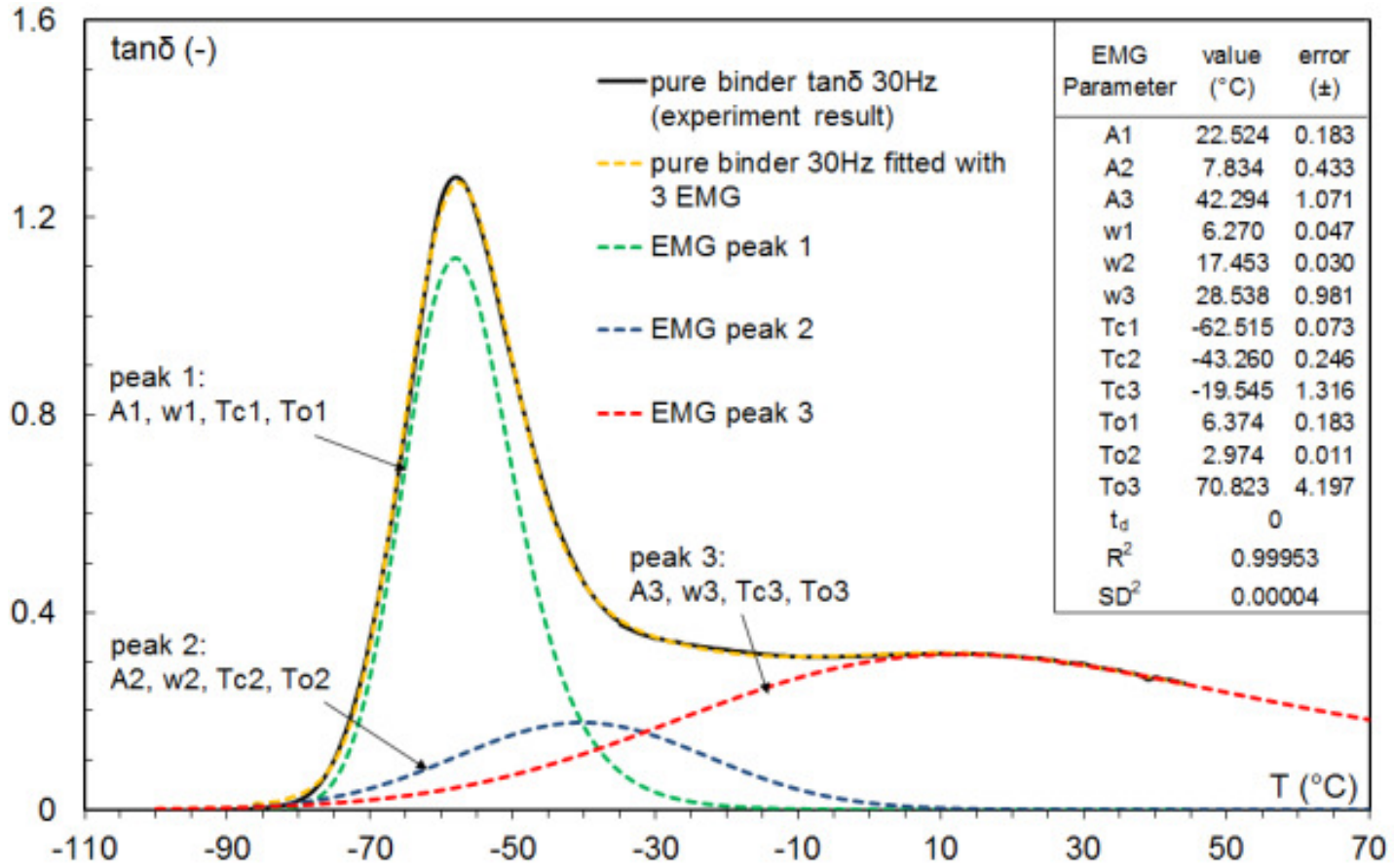

EMG Parameter	value (°C)	error (±)
A1	22.524	0.183
A2	7.834	0.433
A3	42.294	1.071
w1	6.270	0.047
w2	17.453	0.030
w3	28.538	0.981
Tc1	-62.515	0.073
Tc2	-43.260	0.246
Tc3	-19.545	1.316
To1	6.374	0.183
To2	2.974	0.011
To3	70.823	4.197
t_d	0	
R^2	0.99953	
SD^2	0.00004	

Information from EMG parameters

Peak areas A_i

small A is caused by:

(1) – hindrance in mobility

(2) – increase of stiffness (G')

(3) – increase of cross-linking gives rigidity, means a smaller binder part can transform to rubber

Peak temperature Tc_i of Gauss part

It can be interpreted as "Tg" of the relaxation free transition (transition without exponential part) one has a pure Gauss distribution.

Exponential relaxation τ_i

The more exponential part the greater τ_l (To_i) or the more residual internal friction.

Fraunhofer ICT

Influense of particle shape – AP and RDX

SEM analysis reveals that AP-fine and RDX-coarse are not round or less rounded in contrast to AP-coarse and RDX-fine.

AP coarse, rounded

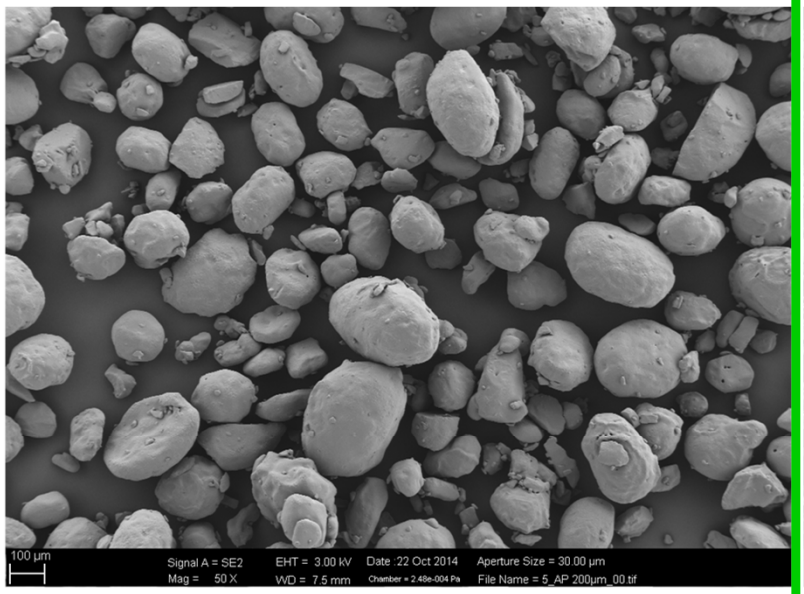

(a)

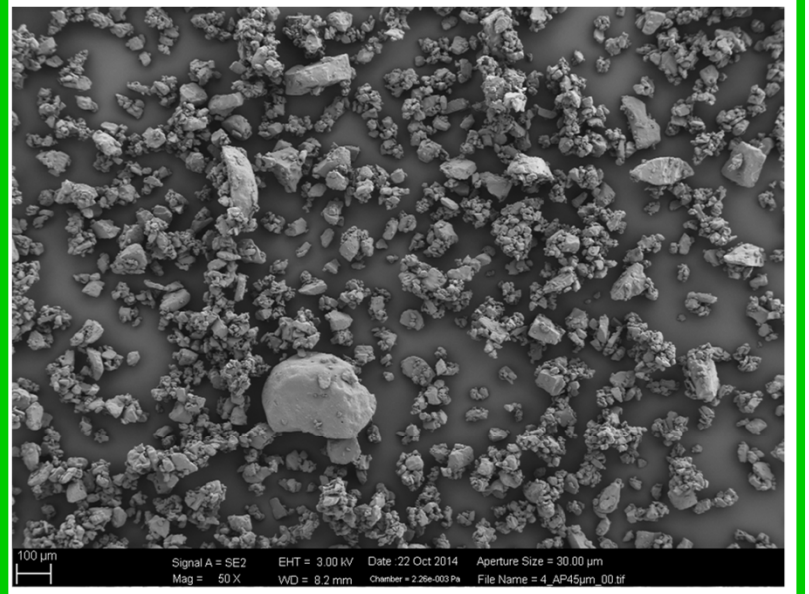

(b)

AP fine, not rounded

RDX coarse, not rounded

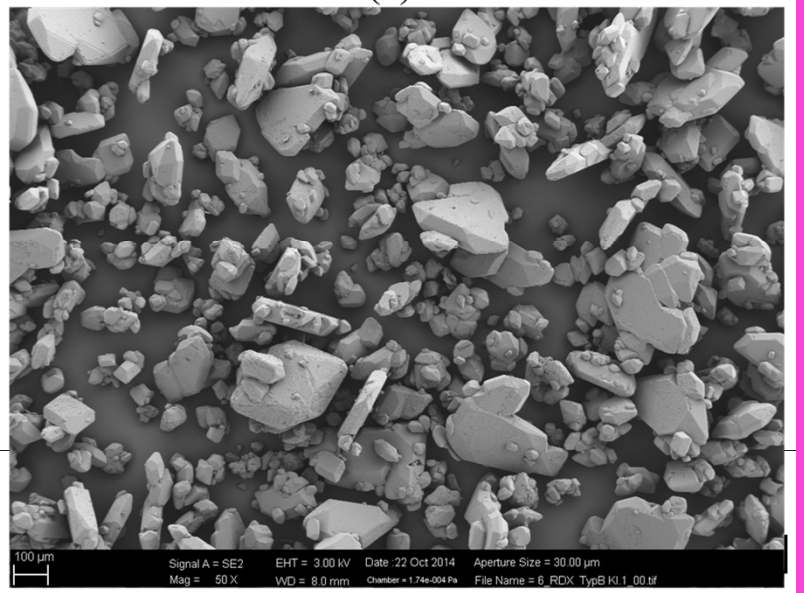

(c)

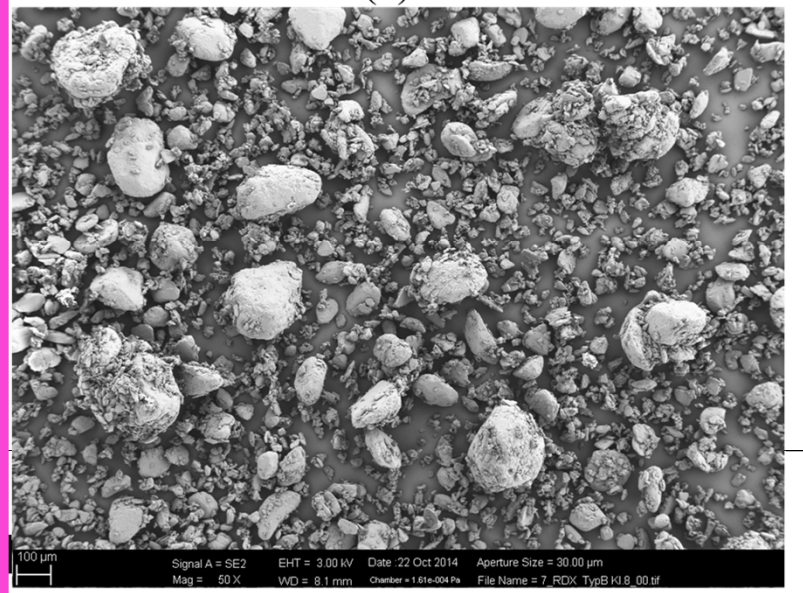

(d)

RDX fine, rounded

Influense of particle shape – Al

SEM analysis reveal that Al coarse and Al-fine are rounded

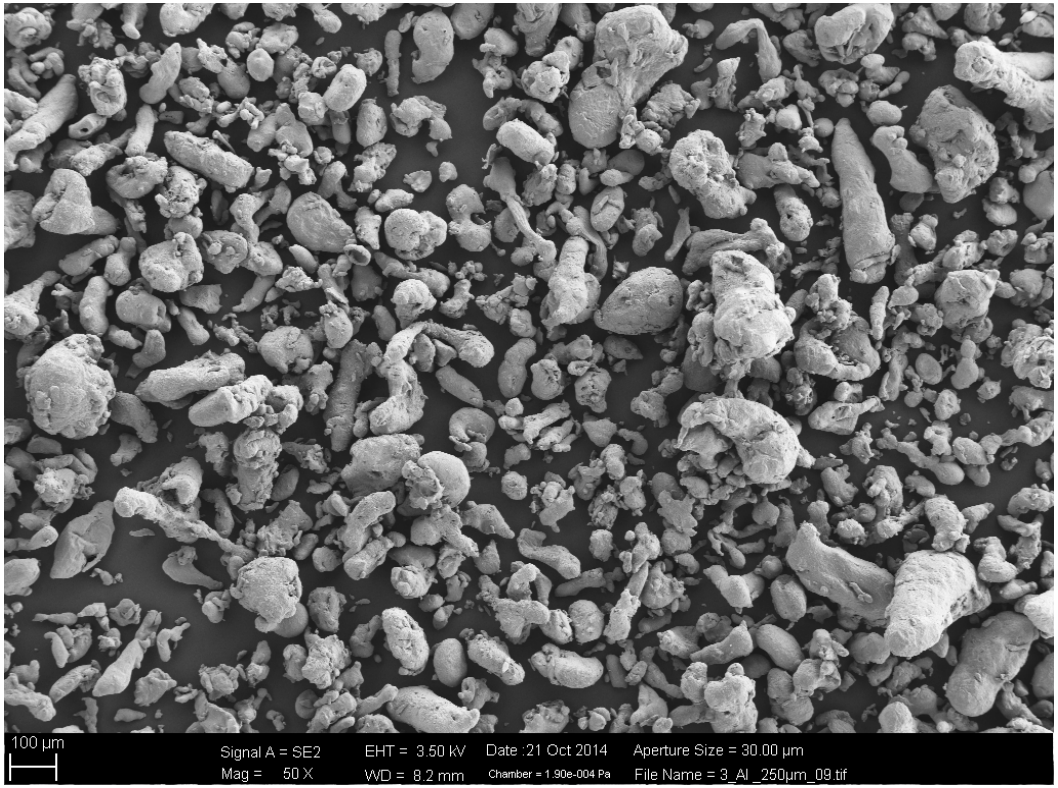

Al coarse,
rounded

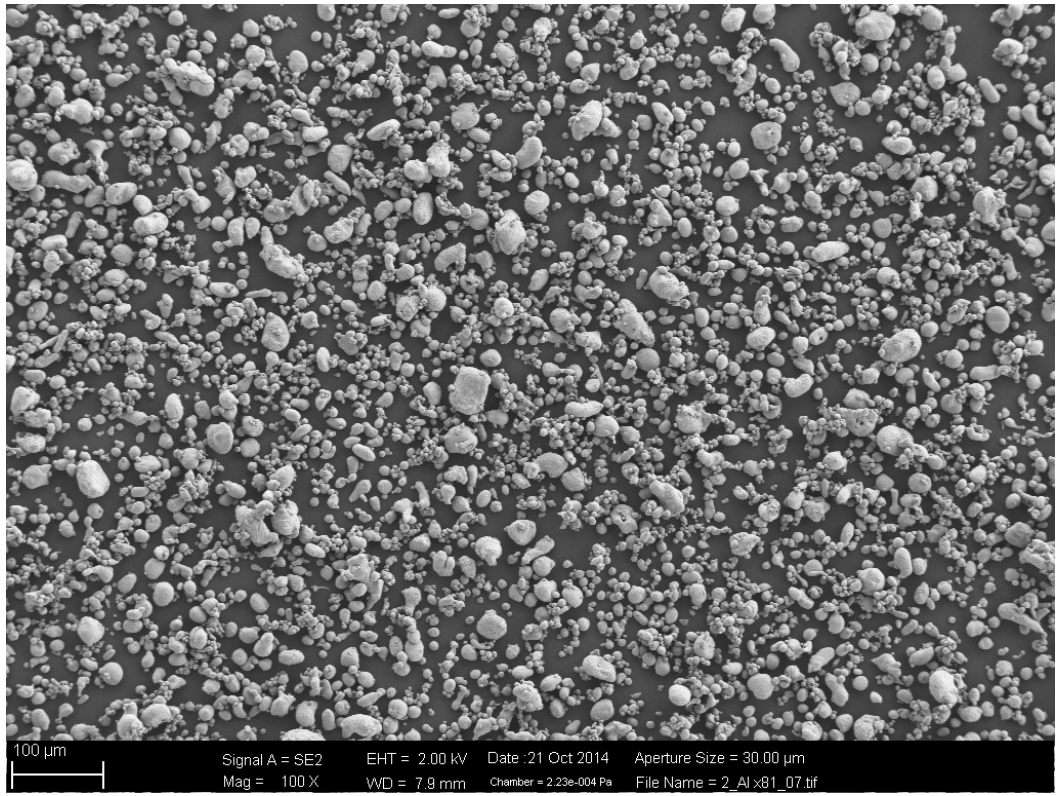

Al fine,
rounded

Generally, rounded particles disturb less the binder structure.
Means, they decrease less the intensity of the loss factor.

Changes in areas A_i of EMG curves at 0.1 Hz, filling is 60 mass-%

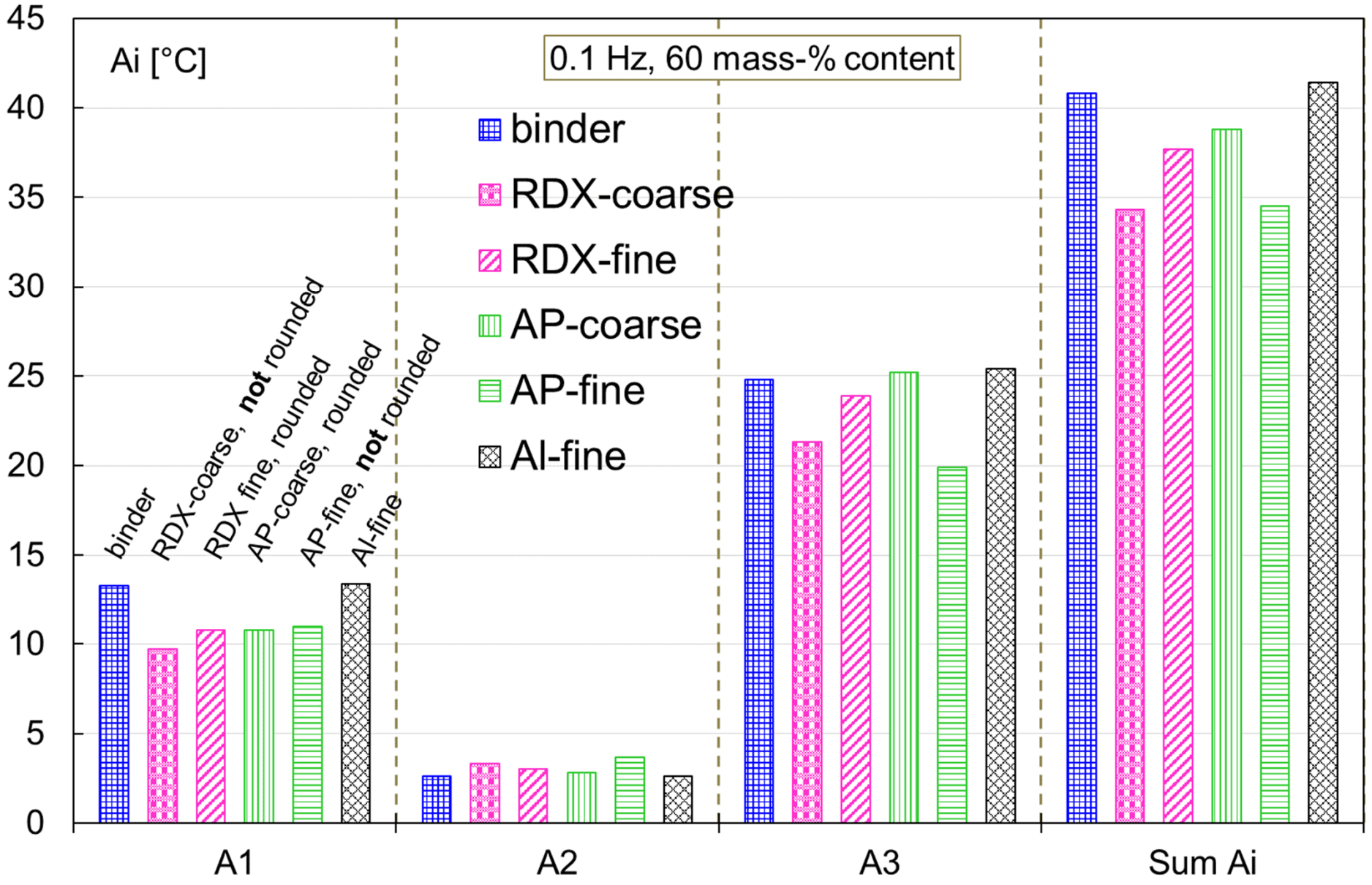

Fraunhofer ICT

Effect of AP on total intensity (sum of areas) of loss factor in glass-rubber transition

	only Binder				60 m.-% AP coarse				60 m.-% AP fine			
f (Hz)	0.1	1	10	30	0.1	1	10	30	0.1	1	10	30
A_1	13.3	16.7	20.3	22.5	10.8	13.5	16.2	18.0	11.0	13.9	17.0	22.5
A_2	2.6	5.6	7.2	7.8	2.8	4.8	8.2	8.3	3.7	7.9	7.6	6.7
A_3	24.8	29.0	39.0	42.3	25.2	30.9	38.7	45.8	19.9	21.3	31.3	34.1
$\sum A_i$	40.8	51.3	66.5	72.7	38.8	49.3	63.2	72.2	34.5	43.1	56.0	63.3
w_1	4.2	5.2	5.6	6.3	4.3	5.2	5.6	6.3	4.5	5.5	6.1	6.7
w_2	2.0	2.7	16.4	17.5	2.1	2.8	17.0	17.5	2.3	3.1	16.5	6.6
w_3	25.3	26.3	26.7	28.5	26.8	27.7	25.5	28.1	24.7	25.6	23.9	30.6
Tc_1	-70	-66	-65	-63	-69	-66	-64	-61	-69	-65	-63	-65
Tc_2	-63	-58	-46	-43	-62	-57	-46	-42	-61	-56	-43	-57
Tc_3	-43	-33	-23	-20	-38	-32	-20	-17	-39	-28	-19	-12
To_1	0.9	1.0	5.6	6.4	0.8	1.0	5.5	6.1	0.9	1.0	5.8	23.8
To_2	9.6	17.1	2.7	3.0	11.4	16.6	3.2	3.0	15.4	26.8	3.3	1.0
To_3	22.3	37.6	60.1	70.8	17.6	35.1	59.3	75.1	20.9	34.5	57.9	66.6

Small to nearly no effect from coarse AP on sum Ai compared to binder

Decrease of sum A_i with fine AP compared to binder

Fraunhofer ICT

Effect of RDX on EMG-parameters of loss factor in glass-rubber transition (GRT)

	only binder				60 m.-% RDX coarse				60 m.-% RDX fine			
f (Hz)	0.1	1	10	30	0.1	1	10	30	0.1	1	10	30
A_1	13.3	16.7	20.3	22.5	9.7	12.1	16.2	19.2	10.8	13.7	17.4	19.4
A_2	2.6	5.6	7.2	7.8	3.3	6.3	7.3	6.1	3.0	5.4	10.1	13.4
A_3	24.8	29.0	39.0	42.3	21.3	22.9	28.6	33.5	23.9	32.5	35.6	37.4
$\sum A_i$	40.8	51.3	66.5	72.7	34.3	41.2	52.2	58.8	37.7	51.6	63.1	70.2
w_1	4.2	5.2	5.6	6.3	4.5	5.5	6.0	6.7	4.3	5.4	6.8	7.6
w_2	2.0	2.7	16.4	17.5	2.2	3.1	17.4	17.3	2.2	3.1	4.1	4.8
w_3	25.3	26.3	26.7	28.5	25.9	27.0	23.8	27.4	26.2	26.7	31.6	34.6
Tc_1	-70	-66	-65	-63	-69	-65	-64	-62	-69	-65	-61	-58
Tc_2	-63	-58	-46	-43	-61	-57	-41	-34	-62	-57	-50	-47
Tc_3	-43	-33	-23	-20	-40	-31	-18	-14	-39	-33	-16	-5
To_1	0.9	1.0	5.6	6.4	0.8	1.0	6.8	8.2	0.8	1.0	1.4	1.5
To_2	9.6	17.1	2.7	3.0	15.5	22.4	3.3	3.2	11.6	17.9	29.3	35.5
To_3	22.3	37.6	60.1	70.8	19.7	32.8	54.4	65.3	19.3	43.3	54.6	60.1

RDX-coarse reduces the intensity of GRT at strainrate hardening compared to binder

RDX- fine changes less in intensity of GRT at strainrate hardening compared to binder

Tc_1 but especially Tc_3 are shifted to higher temp. The shift is larger at high strainrate, especially with RDX-fine compared to binder

Fraunhofer ICT

Effect of Al-fine on EMG-parameters of loss factor in glass-rubber transition

	only binder				60 mass-% Al fine			
f (Hz)	0.1	1	10	30	0.1	1	10	30
A_1	13.3	16.7	20.3	22.5	13.4	14.9	17.7	21.2
A_2	2.6	5.6	7.2	7.8	2.6	5.2	7.5	6.5
A_3	24.8	29.0	39.0	42.3	25.4	35.6	48.2	49.8
$\sum A_i$	40.8	51.3	66.5	72.7	41.4	55.7	73.4	77.4
w_1	4.2	5.2	5.6	6.3	4.2	5.2	5.1	6.0
w_2	2.0	2.7	16.4	17.5	1.7	2.9	21.1	20.0
w_3	25.3	26.3	26.7	28.5	25.8	27.0	30.1	34.2
Tc_1	-70	-66	-65	-63	-70	-66	-65	-63
Tc_2	-63	-58	-46	-43	-63	-58	-49	-39
Tc_3	-43	-33	-23	-20	-41	-30	-20	-11
To_1	0.9	1.0	5.6	6.4	0.8	1.0	6.6	7.5
To_2	9.6	17.1	2.7	3.0	9.9	16.0	3.0	3.1
To_3	22.3	37.6	60.1	70.8	21.0	35.8	59.3	56.6

Area A_3 of second evident peak:

Al particles have a larger effect on increase of area A_3 than the AP and RDX have.

Increase of deformation frequency amplifies this effect.

From molecular dynamics studies it is known, that Al has a stronger **intermolecular interaction with HTPB than** AP. Therefore **more mobility hindrance** of HTPB chains, this increases the range of the polymer shell around Al particles, therefore a higher intensity in loss factor.

Al has always OH-groups on its surface, therefore:

(1) Reaction with NCO, which can promote more free polymer chains around Al – reptation possible

(2) chemical bonding of the Al particle with the binder network via NCO enlarges the polymer shell around the Al particle, whereby the area A_3 increase.

(3) Significant increase of maximum temperature Tc_3 (Gauss peak of second evident peak or the third peak in EMG)

Conclusions on interactions filler - binder

AP and RDX cause more changes in intensity of first evident peak of loss factor than AL.

The peak temperature in first maximum is changed not much (only a bit lowered) by any of the fillers at all concentrations.
AL changes it least of all fillers (always in comparison to unfilled binder).

The changes in peak temperature of second peaks are clearly larger, especially with increasing deformation frequency.

AP-fine stronger decrease of tanδ intensity compared to AP-coarse.
RDX-fine less decreases of tanδ intensity compared to RDX-coarse.

There is indication that particle shape has an influence.
The more rounded particles have a less hindrance effect on molecular mobility, and reduce the tanδ intensity less than not rounded particles.

Change in loss factor intensity and temperature shifts indicate that AL particles have a stronger molecular interaction with the binder than AP and RDX.
It seems AL is bonded to the binder network via isocyanate coupling, because on AL surfaces always OH groups are present.

Fraunhofer ICT